Int. J. Electrochem. Sci., 17 **(2022)** Article Number: 220423, doi: 10.20964/2022.04.47

International Journal of
ELECTROCHEMICAL
SCIENCE
www.electrochemsci.org

Development of Nanostructured Enzymic Amperometric Biosensor based on Gold Nanoparticles for Detection of Pyruvate in Natural Samples

Meiling Shao[*], *Zhan Shi, Sanxu Pu, Jiashu Sun, Yihui Bai*

College of Chemistry and Chemical Engineering, Shangqiu Normal University, Shangqiu 476000, China
[*]Correspondings E-mail: shao_mei_ling@sina.com

Received: 30 December 2021 / *Accepted:* 11 February 2022 / *Published:* 4 March 2022

The goal of this work was to create an enzymatic nanostructured-based amperometric biosensor for pyruvate detection in blood serum samples. The biosensor was prepared by electrodeposition of Au@CNTs nanocomposite on a glassy carbon electrode and immobilization of the pyruvate oxidase (PyOx) on nanocomposite (PyOx/Au@CNTs/GCE). The structural studies using XRD and SEM indicated the metallic Au NPs were effectively decorated on the CNTs surface and Au@CNTs nanocomposite electrodeposited on the GCE surface. EIS analyses also confirmed the covalent binding of PyOx molecules onto the Au@CNTs surface. CV, DPV and amperometry measurements showed that the PyOx/Au@CNTs/GCE had good specificity, sensitivity and stability to determination pyruvate, and a linear range of 10 to 480 µM, detection limit of 5 nM and sensitivity of 0.12482 µA/µM were obtained for the developed pyruvate biosensor. Moreover, comparison of the results obtained of developed biosensor to those of previously reported pyruvate biosensor systems demonstrated a comparable or better linear range and detection limit of PyOx/Au@CNTs/GCE that is associated with the synergistic catalytic effect of Au NPs and CNTs and immobilized PyOx molecules. The practicality and precision of the biosensor were examined for the determination level of pyruvate in blood serum of healthy adults as real samples and results showed good agreement between the amperometry and ELISA techniques, and also acceptable accuracy (RSD from 2.11% to 4.14%). These findings indicate that PyOx/Au@CNTs/GCE as a reliable pyruvate biosensor can be used for clinical diagnosis.

Keywords: Enzymatic Biosensor; Amperometry; Pyruvate; Electrodeposition; Nanocomposite; CNTs; Specificity

1. INTRODUCTION

Pyruvate ($C_3H_3O_3$) also known as 2-oxopropanoate is an organic compound that probably occurs in all living cells [1-3]. It is a versatile biological molecule that consists of three carbon atoms

and two functional groups - a carboxylate and a ketone group [4, 5]. This biological molecule is involved in a number of key biochemical processes, including gluconeogenesis, which is the synthesis of glucose, as well as the synthesis of other key biochemicals [6, 7]. It is the output of the anaerobic metabolism of glucose in the cytoplasm known as glycolysis. In glycolysis reactions, one glucose molecule breaks down into two pyruvate molecules, which supplies energy to living cells through the Krebs cycle in aerobic respiration [8]. The other function of pyruvate is to serve as a transporter of carbon atoms into the mitochondrion for complete oxidation into carbon dioxide [9, 10].

The normal range of pyruvate values in blood lies between 40 and 120 μM, and between 40 and 100 μM in human serum [11]. Pyruvate deficiency is caused when the red blood cells break down too easily, resulting in a low level of these cells known as hemolytic anemia [12]. Diabetes, cirrhosis, cardiovascular diseases, and severe brain abnormalities are several disorders caused by pyruvate deficiency in the human body [13, 14]. Moreover, pyruvate kinase deficiency is caused by mutations in the PKLR gene that as an active gene in the liver and in red blood cells provides instructions for making an enzyme called pyruvate kinase, which is involved in a critical energy-producing process known as glycolysis [15].

Therefore, determination of the pyruvate level in natural and biological samples is an important factor in providing information about disease mechanisms and protein-drug interactions [16, 17]. Accordingly, much research has been conducted on various methods to identify and determine the pyruvate level in biological samples. These methods include spectrophotometry [18], Q-PCR assay [19], gas chromatography [20], reversed-phase high-performance liquid chromatography [21], fluorimetric assay [22], capillary electrophoresis [23], and electrochemical biosensors [13, 24]. However, these methods are expensive and require pre-treatment steps and skilled workers to operate with large volumes of clinical samples [25]. Among them, electrochemical biosensors as low-cost and simple analytical devices offer an interesting alternative to overcome these problems. Electrochemical biosensors use biological molecules to enhance the sensitivity and selectivity [26-29], and additionally, the use of nanostructure in electrode architecture can increase the stability and biocompatibility of biosensors [30-34]. Therefore, this study was carried out to develop an enzyme nanostructured based amperometric biosensor using PyOx/Au@CNTs/GCE for the detection of pyruvate in blood serum samples.

2. EXPERIMENTAL

2.1. Synthesis and Modification of PyOx/Au@CNTs/GCE

Before modification by the GCE, the GCE (3 mm in diameter, Tianjin Aida Hengsheng Technology Development Co., Ltd., China) was carefully polished with alumina powder (0.05 μm, 99%, Hebei Suoyi New Material Technology Co., Ltd., China) for 10 minutes, and cleaned with deionized (DI) water. Then, it was sonicated in a mixture of HNO_3 (65%, Merck, Germany), ethanol (99%, Shandong Dexiang International Trade Co., Ltd., China) and DI water (v: v 1:1) for 5 minutes to remove alumina particles from the surface. The electrodeposition was used for synthesizing Au

nanoparticles on GCE using an electrochemical working station (CorrTest, Wuhan Corrtest Instruments Corp., Ltd., China) in a conventional three-electrode electrolytic cell consisting of the GCE as working electrode, Ag/AgCl as reference electrode and Pt wire as counter electrode in an electrolyte prepared from 0.1 mM $HAuCl_4$ (99%, Sigma-Aldrich) solution containing dispersed 1 g/l CNTs (99%, Jiaxing ACG Composites Co., Ltd., China) in 0.1 M phosphate Buffered Saline (PBS, Sigma-Aldrich) solution (pH 8.5) [35]. CV electrodeposition was conducted on a potential range from 1.3 to 0.7 V at a scan rate of 20 mV/s during 25 cycles. For immobilization of the PyOx, 10 µL of 50 µM PyOx (Sigma-Aldrich) solution was dropped onto the Au@CNTs modified GCE surface and stored at 4°C for 12 hours [36]. Before electrochemical measurements, the prepared PyOx/Au@CNTs/GCE was washed thoroughly with 0.1 M PBS (pH 7) to remove unbounded PyOx and then kept in a humid chamber at room temperature.

2.2. Characterization

An X-ray diffractometer (XRD; D8 advance; Bruker AXS, Madison, WI) was used for the crystallographic analysis of samples. A Scanning electron microscope (SEM, Zeiss ULTRA plus with Charge Compensation) was applied for morphological analyses of prepared nanostructures. Electrochemical impedance spectroscopy (EIS), cyclic voltammetry (CV), differential pulse voltammetry (DPV) and amperometry measurements were carried out using the electrochemical working station where the bare and modified GCE act as working electrodes. Electrolyte for electrochemical studies were included 5mM $[Fe(CN)6]^{3-/4-}$ (≥99%, Sigma-Aldrich), and 0.1 M PBS (pH 7) containing 1mM $MgCl_2$ (≥98%, Merck, Germany), 1 µM flavin adenine dinucleotide (FAD, ≥95%, Sigma-Aldrich), 10 mM thiamine pyrophosphate (TPP, ≥95%, Sigma-Aldrich) and 0.1M pyruvate (≥99%, Sigma-Aldrich) solution.

2.3 Analysis of real samples

Blood samples from healthy adult volunteers aged 30 to 70 years were taken from local hospitals (Beijing United Family Hospital, Beijing, China). The samples were left for 60 minutes at room *temperature*, and then centrifuged for 6 minutes at 2000 rpm. The obtained supernatants were taken and stored at 5°C until used to prepare the electrolyte as real samples with 0.1 M PBS pH 7.0 containing 1 mM $MgCl_2$, 1 µM FAD and 10 mM TPP. The amperometric measurements using PyOx/Au@CNTs/GCE were employed for the determination of the level of pyruvate in prepared real samples at a potential of 0.5 V at a rotating speed of 1500 rpm. The Pyruvate Assay Kit (ELISA, ab65342, and detection range from 1 µM to 200 µM, abcam, USA) was also used for the determination of the Pyruvate level in blood serum samples.

3. RESULTS AND DISCUSSION

CNTs/GCE and Au@CNTs/GCE morphologies were investigated using SEM imaging. Figure 1a shows the SEM image of the CNTs/GCE that presents the three-dimensional network structure of

the CNTs layer without aggregation deposited on the GCE surface, implying that the CNTs were homogeneously dispersed on the electrode surface with an average diameter of 45 nm. The CNTs network plays an important role in electron transfer in electrochemical reactions because of its high porosity and large surface area. Figure 1b displays the SEM image of Au@CNTs/GCE that reveals the Au NPs electrodeposited on the CNTs in a spherical shape with an average diameter of ~ 30 nm. As observed, the Au NPs on CNTs network enhance the porosity and increase the target molecular adsorption capacity of the modified electrode.

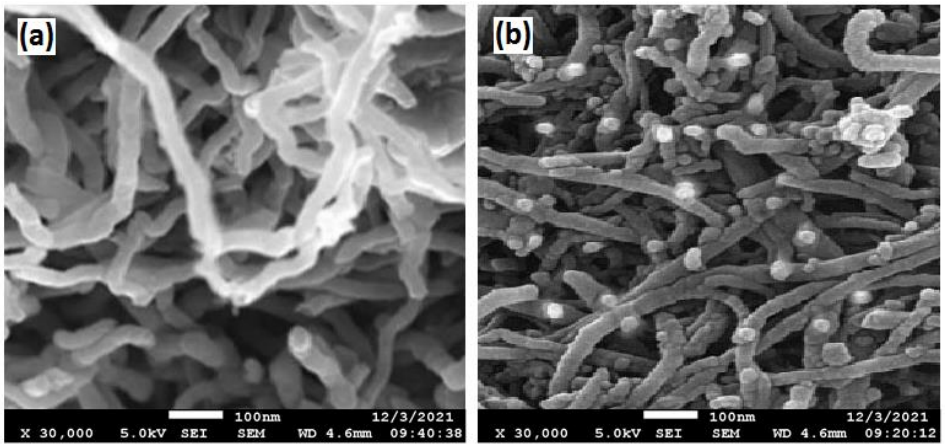

Figure 1. SEM image of (a) CNTs/GCE and (b) Au@CNTs/GCE

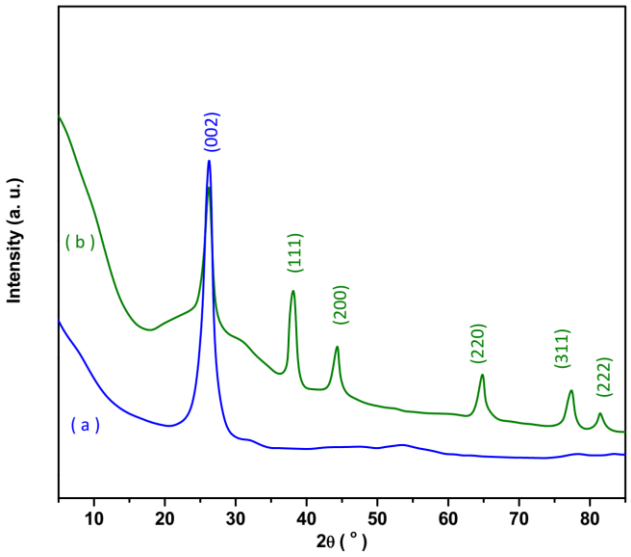

Figure 2. XRD pattern of (a)CNTs and (b) Au@CNTs on the GCE surface

The crystallization of electrodeposited CNTs and Au@CNTs on the GCE surface was explored by XRD. As observed from Figures 2a and 2b, the XRD pattern of CNTs and Au@CNTs shows a

strong diffraction peak at 26.22° which is related to the (002) plane of the graphite (JCPDS Card No. 65-6212). The XRD patterns of Au@CNTs display several diffraction peaks at 38.14°, 44.27°, 64.75°, 77.39°,and 81.50° which are associated with (111), (200), (220), (311) and (222) planes of metallic Au NPs with face-centered cubic (fcc) structure (JCPDS No. 04-0784), respectively, indicating that the metallic Au NPs are effectively decorated on the CNTs surface.

Figure 3 shows the EIS analyses of GCE, CNTs/GCE, Au@CNTs/GCE and PyOx/Au@CNTs/GCE in 5 mM $[Fe(CN)6]^{3-/4-}$] at a potential of 0.2 V in a frequency range of 10^{-2} Hz to 10^{4} Hz. As observed, there is an incomplete semicircle in the high frequency region of EIS where the diameter of the semicircles is associated with the charge transfer resistance (R_{ct}). It can be found that the charge transfer resistance can represent the interfacial properties of the electrode, which are controlled by the electrode surface modification [37]. The R_{ct} value of GCE is small, and a decrease in R_{ct} can be observed following the order: GCE > CNT/ GCE > PyOx/Au@CNTs/GCE > Au@CNTs/GCE. The R_{ct} value is decreased by modification with CNTs due to the high surface area of the CNTs and to the presence of defects and withdrawn electrons to improve the kinetics of diffusion and transfer [38]. After the incorporation of Au NPs onto CNTs an even greater decrease of R_{ct} is obtained, demonstrating that Au NPs have excellent electroconductibility and can accelerate the electron-transfer process [39]. For PyOx/Au@CNTs/GCE samples, it is observed that the R_{ct} value is greater than Au@CNTs/GCE because of the covalent binding of PyOx molecules onto the Au@CNTs surface [24], and biomolecules are non-conductive and can restrain electron transfer [40, 41].

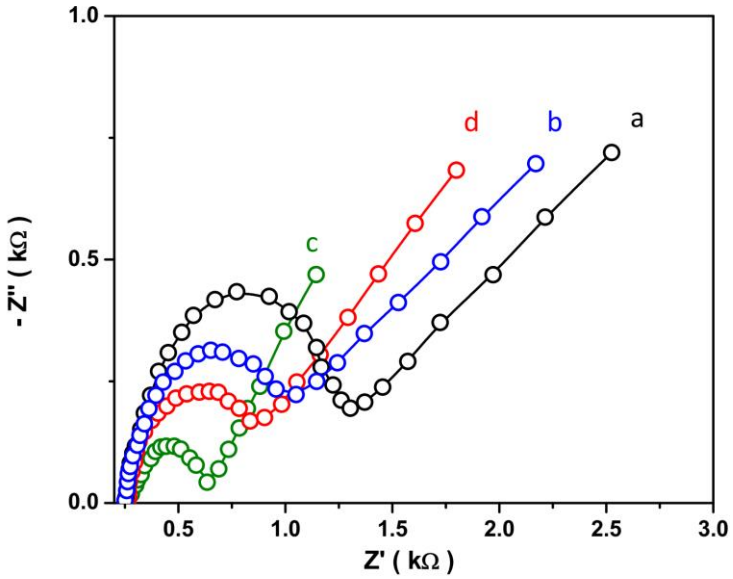

Figure 3. EIS analyses of (a) GCE, (b) CNTs/GCE, (c) Au@CNTs/GCE and (d) PyOx/Au@CNTs/GCE in 5 mM $[Fe(CN)6]^{3-/4-}$] at the potential of 0.2 V in a frequency range of 10^{-2} Hz to 10^{4} Hz.

Figure 4 shows the voltammometric response of GCE, CNTs/GCE, Au@CNTs/GCE and PyOx/Au@CNTs/GCE in 5 mM $[Fe(CN)6]^{3-/4-}$] at a potential range of -0.2 V to 0.6 V at 20mV/s scan rate. It can be found that the $[Fe(CN)6]^{3-/4-}$ redox currents on bare GCE is smaller than those on the other electrodes and an increase in $[Fe(CN)6]^{3-/4-}$ redox currents can be observed following the order:

GCE < CNT/ GCE < PyOx/Au@CNTs/GCE < Au@CNTs/GCE. Moreover, the separation of the two peak potentials for a reversible redox of $[Fe(CN)6]^{3-/4-}$ (ΔEp) is decreased in CNTs/GCE and Au@CNTs/GCE because of the great electron transfer ability of CNTs and Au NPs [42]. The redox currents are further enhanced on Au@CNTs/GCE compared with those on other electrodes, which confirms that to the presence of Au NPs in the Au@CNTs nanocomposite effectively facilitates electron transfer [42, 43]. For PyOx/Au@CNTs modified electrode, a decrease in the peak current toward Au@CNTs/GCE occurs which associated with the electrostatic repulsive force between the negatively charged PyOx molecules on the electrode and $[Fe(CN)6]^{3-/4-}$ in the electrolyte [44, 45]. It confirms the proper immobilization of PyOx molecules onto Au@CNTs nanocomposite.

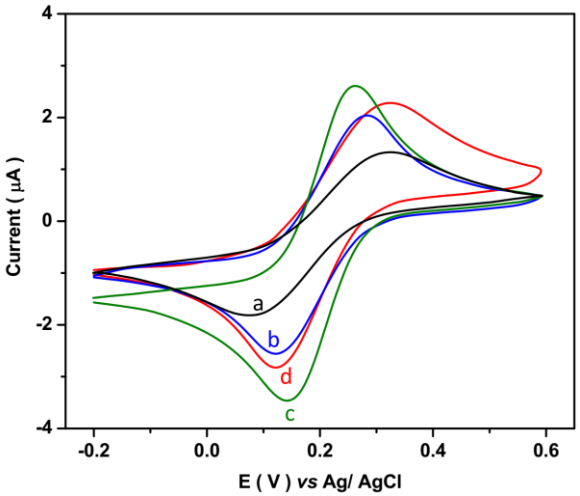

Figure 4. The voltammometric response of (a) GCE, (b) CNTs/GCE, (c) Au@CNTs/GCE and (d) PyOx/Au@CNTs/GCE in 5 mM $[Fe(CN)6]^{3-/4-}$] at the potential range of -0.2 V to 0.6 V at scan rate of 20mV/s.

Figure 5 shows the DPV response of GCE, CNTs/GCE, Au@CNTs/GCE and PyOx/Au@CNTs/GCE in 100 ml of 0.1 M PBS (pH 7) containing 0.05 ml each of 1 mM $MgCl_2$, 1 µM FAD and 10 mM TPP at a potential range of 0.05 V to 1.25 V at a 20 mV/s scan rate. Before the addition of pyruvate solution, it is observed that GCE and CNTs/GCE do not show any peaks, and Au@CNTs/GCE and PyOx/Au@CNTs/GCET show an anodic peak at 0.5 V that is related to the oxidation Au^0 into Au^+ [46-48]. After addition of 0.5ml of 0.1M pyruvate solution, GCE and CNTs/GCE do not show any obvious peak, and Au@CNTs/GCE do not exhibit any prominent reduction and oxidation peak. PyOx/Au@CNTs/GCE displays significantly clear increase in oxidation peak, confirming the succsecful immobilization of PyOx molecules onto Au@CNTs/GCE, and sensitive response of PyOx/Au@CNTs/GCE to determination pyruvate. PyOx is a tetrametric flavoenzyme with strong binding sites with FAD, TPP and magnesium as cofactors that catalyse the reaction [49]. This enzyme utilizes cofactors for the oxidative decarboxylation of pyruvate [50]. These cofactors are required for the enzymatic reaction of pyruvate, and the primary substrate of the enzyme

does not interfere with the generated signal of the voltage in electroactivity on the electrode surface [51]. According to reactions 1 and 2, in the presence of pyruvate oxidase, pyruvate and phosphate are catalytically oxidized to produce acetylphosphate and hydrogen peroxide. The hydrogen peroxide may be oxidized on the working electrode. the current is attributed to the concentration of pyruvate [26].

$$\text{Pyruvate} + \text{Phosphate} + O_2 \xrightarrow{\text{PyOx}} \text{Acetylphosphate} + CO_2 + H_2O_2 \quad (1)$$

$$H_2O_2 \rightarrow O_2 + 2H^+ + 2e^- \quad (2)$$

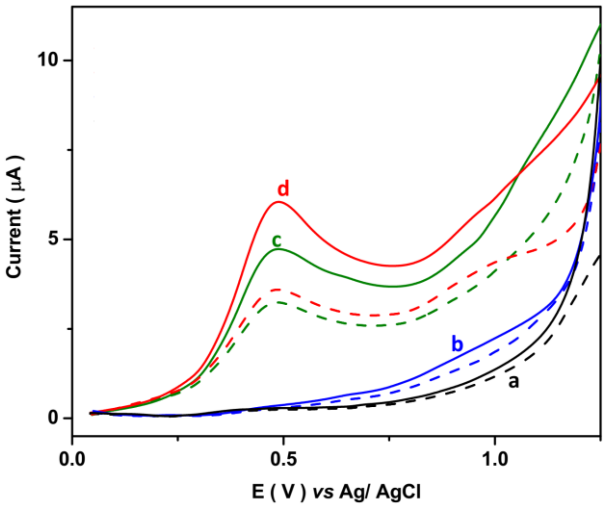

Figure 5. DPV response of (a) GCE, (b) CNTs/GCE, (c) Au@CNTs/GCE and (d) PyOx/Au@CNTs/GCE in 100 ml of 0.1 M PBS (pH 7) containing 0.05 ml of each of 1 mM $MgCl_2$, 1 µM FAD and 10 mM TPP at the potential range of 0.05 V to 1.25 V at a scan rate of 20 mV/s (before and after addition 0.5 ml of 0.1 M pyruvate solution specified by dashed line and solid line, respectinely).

Furthermore, the stability of the electrochemical response of Au@CNTs/GCE and PyOx/Au@CNTs/GCE was investigated in 100 ml of 0.1 M PBS (pH 7) containing 0.5 ml of 0.1 M pyruvate solution, 0.05 ml each of 1 mM $MgCl_2$, 1 µM FAD and 10 mM TPP at the potential range of 0.05 V to 1.25 V at a scan rate of 20 mV/s. Figure 6 shows the intital DPV response and the obtained DPV response after successive 50 sweeps, which illustrated to 4.5% and 13.4% decrease for voltammometric response of Au@CNTs/GCE and PyOx/Au@CNTs/GCE, respectively. It is indicated to greater stability of PyOx/Au@CNTs/GCE because of perfect biocompatibility of Au NPs [52]. If the enzyme were covalently attached to the Au@CNTs nanocomposite, reasonable for greater stability could be achieved [24, 53]. Thus, the following electrochemical studies were conducted on PyOx/Au@CNTs modified GCE as a sensitive and stale electrode.

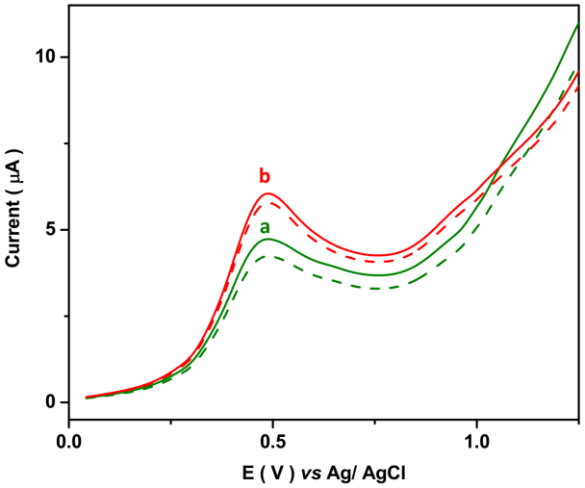

Figure 6. DPV response of (a) Au@CNTs/GCE and (b) PyOx/Au@CNTs/GCE in 100 ml of 0.1 M PBS (pH 7) containing 0.5 ml of 0.1 M pyruvate solution, 0.05 ml each of 1 mM $MgCl_2$, 1 µM FAD and 10 mM TPP at the potential range of 0.05 V to 1.25 V at a scan rate of 20 mV/s (first CV solid line and 50^{th} CV dashed line).

Figure 7 shows the amperometric response and obtained calibration curve of PyOx/Au@CNTs/GCE to successive addition of 30 µM pyruvate solution in 100 ml of 0.1M PBS (pH 7) containing 0.05 ml of each of 1 mM $MgCl_2$, 1 µM FAD and 10 mM TPP at a potential of 0.5 V at a rotating speed of 1500 rpm. It is observed that the modified electrode demonstrates a relatively fast response to each addition of pyruvate solution, and the electrocatalytic *response shows* a linear increase with successive addition of pyruvate from 10 to 480 µM in the electrochemical cell. The calibration curve obtained from amperometric response reveals *that* detection limit and sensitivity of the developed pyruvate biosensor are 5 nM and 0.12482 µA/µM, respectively. Table 1 compares the results obtained of the developed biosensor in this study to those of previously reported pyruvate biosensor systems. It is demonstrated to have a comparable or better linear range and detection limit than PyOx/Au@CNTs/GCE to determine pyruvate that it is associated with the synergistic catalytic effect of Au NPs and CNTs and immobilized PyOx molecules. PyOx catalyzes the oxidative decarboxylation of pyruvate in the presence of phosphate and oxygen [54], and the Au NPs and CNTs act as good conductive and high biocompatible nanostructures attracted significant attention for enzyme immobilization owing to their large surface area [55-57].

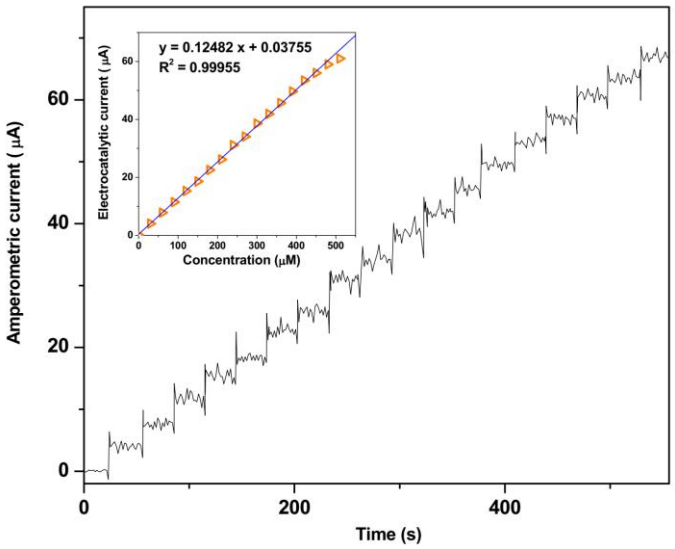

Figure 7. (a) amperometric response and (b) obtained calibration curve of PyOx/Au@CNTs/GCE to successive addtion of 30 µM pyruvate solution in 100 ml of 0.1 M PBS (pH 7) containing 0.05 ml of each of 1 mM $MgCl_2$, 1 µM FAD and 10 mM TPP at the potential of 0.5 V at rotating speed of 1500 rpm.

Table 1. Comparison between the results obtained of developed biosensor in this study to those of previously reported pyruvate biosensor systems.

Electrodes	Technique	Detection limit (nM)	Linear range (µM)	Ref.
PyOx/Au@CNTs/GCE	AMP	5	1 to 480	This work
PyOx/ Polytyramine/Pt/GCE	AMP	50000	100 to 3000	[26]
Lactate dehydrogenase/poly (vinyl alcohol/ Au NPs/graphene oxide	AMP	8.69 0	5 to 140	[27]
Os(bipy)2pyCl-modiFed pyrrole/thiophene platinized glassy-carbon electrode	AMP	26	20 to 3000	[30]
Poly(neutral red) /carbon film electrode	AMP	34000	90 to 600	[31]
Carbon fiber bundle electrode	LSV	8000	10 to 1000	[33]
Fullerene–C60–MWCNT/GCE	DPV	0.1	0.002 to 0.055	[32]
Ag−rGO	DPV	0.5	0.025 to 1.43	[58]
CoOx(OH)y/ITO	CV	550	1 to 1910	[59]
Hanging mercury drop electrode	SWAdSV	6.12	4 to 36	[60]
Hanging mercury drop electrode	DPAdSV	0.112	4 to 36	[60]
Tris(2,2′-bipyridiyl)ruthenium(III) ($Ru(bpy)_3^{3+}$)	CL	21	0.754 to 11.81	[61]

AMP : Amperometry, LSV: Linear sweep voltammetry; SWAdSV: Square-wave adsorptive stripping voltammetry; DPAdSV: Differential pulse adsorptive stripping voltammetry; CL: Chemiluminescence.

The specificity of PyOx/Au@CNTs/GCE to the determination of pyruvate was also explored in the presence of several blood components as interfering substances through amperometric experiments in 100 ml of 0.1M PBS containing 0.05ml of each of 1 mM $MgCl_2$, 1 µM FAD and 10 mM TPP at a potential of 0.5 V at a rotating speed of 1500 rpm. The results of amperometric experiments are presented in Table 2 which indicates a significant amperometric response of PyOx/Au@CNTs/GCE to the addition of pyruvate, and negligible responses of proposed biosensor to addition two-fold of

interfering substances in electrochemical cell. Thus, the presented components in Table 2 had no effect on biosensor response, and the proposed procedure can be considered to be specific. The specificity of PyOx/Au@CNTs/GCE is related to PyOx, which as an Escherichia coli peripheral membrane flavoprotein catalyzes the oxidative decarboxylation of pyruvate [62].

Table 2. The amperometric response of PyOx/Au@CNTs/GCE in 100 ml of 0.1 M PBS (pH 7) containing 0.05 ml of each of 1 mM $MgCl_2$, 1 µM FAD and 10 mM TPP at the potential of 0.5 V at rotating speed of 1500 rpm for successive addition of 50 µM pyruvate and 100 µM interfering substances.

Substance	**Added (µM)**	**Amperometric response (µA) at 0.5V**	**RSD (%)**
Pyruvate	50	6.2511	±0.1207
Ascorbic Acid	100	0.1212	±0.0185
Uric Acid	100	0.2208	±0.0218
Lactic acid	100	0.7200	±0.0529
Urea	100	0.2305	±0.0112
Glucose	100	0.1109	±0.0225
Nitrite	100	0.1448	±0.0212
Valine	100	0.0851	±0.0088
Lycine	100	0.0964	±0.0057
Phenylalanine	100	0.0872	±0.0082
Folic acid	100	0.1610	±0.0104
Ca^{2+}	100	0.1063	±0.0238
Cu^{2+}	100	0.3208	±0.0282
K^{+}	100	0.0729	±0.0069
Na^{+}	100	0.0841	±0.0043
SO_4^{2-}	100	0.0807	±0.0033
Zn^{2+}	100	0.1217	±0.0128
Mg^{2+}	100	0.1551	±0.0182
Al^{3+}	100	0.6102	±0.0422

The practicality and precision of the developed electrochemical biosensor were tested for the determination of pyruvate in the blood serum of healthy adults as real samples. Table 3 presents the results of determinations of the level of pyruvate using the amperometry and ELISA techniques which demonstrate good agreement between the two techniques, and also acceptable accuracy (RSD from 2.11% to 4.14%). These findings show that PyOx/Au@CNTs/GCE as a reliable pyruvate biosensor can be used for clinical diagnosis.

Table 3. The results of determinations of level of pyruvate in blood serum samples using the amperometry and ELISA techniques.

Age group	Pyruvate level in blood serum samples ((µM)							
	Amperometry using PyOx/Au@CNTs/GCE				ELISA			
	Male	RSD (%)	Female	RSD (%)	Male	RSD (%)	Female	RSD (%)
30-40	61.2	±3.55	48.3	±3.73	59.9	±2.21	49.1	±3.21
40-50	69.1	±3.29	77.5	±2.11	70.0	±3.19	77.8	±4.11
50-60	81.4	±4.07	69.5	±3.10	80.9	±3.77	70.2	±3.93
60-70	59.6	±4.14	70.3	±4.08	60.1	±3.64	69.2	±3.72

4. CONCLUSION

In the present work, PyOx/Au@CNTs/GCE as an enzymatic nanostructured biosensor was prepared by electrodeposition of Au@CNTs nanocomposite on GCE and immobilization of PyOx on the nanocomposite. The results of structural analyses indicated that the metallic Au NPs were effectively decorated on the CNTs surface and Au@CNTs nanocomposite electrodeposited on the GCE surface. EIS analyses also confirmed the covalent binding of PyOx molecules onto the Au@CNTs surface. Electrochemical measurements showed that the PyOx/Au@CNTs/GCE had good specificity, sensitivity and stability to determination pyruvate, and its linear range, detection limit, and sensitivity were obtained at 10 to 480 µM, 5 nM and 0.12482µA/µM, respectively. The practicality and precision of the biosensor were examined for the determination level of pyruvate in blood serum of healthy adults as real samples and results showed good agreement between the amperometry and ELISA techniques, and also acceptable accuracy. These findings indicate that PyOx/Au@CNTs/GCE as a reliable pyruvate biosensor can be used for clinical diagnosis.

ACKNOWLEDGEMENT
This work was supported by the National Natural Science Foundation of China (NSFC) (grant number 21905168), and the Science and Technology Fund of Henan Province (20A430021).

References

1. Y. Zhang, P.V. Taufalele, J.D. Cochran, I. Robillard-Frayne, J.M. Marx, J. Soto, A.J. Rauckhorst, F. Tayyari, A.D. Pewa and L.R. Gray, *Nature metabolism*, 2 (2020) 1248.
2. H. Maleh, M. Alizadeh, F. Karimi, M. Baghayeri, L. Fu, J. Rouhi, C. Karaman, O. Karaman and R. Boukherroub, *Chemosphere*, (2021) 132928.
3. M. Khosravi, *Journal of Eating Disorders*, 8 (2020) 1.
4. A. Medghalchi, M. Akbari, Y. Alizadeh and R.S. Moghadam, *Journal of current ophthalmology*, 30 (2018) 353.
5. W. Liu, Y. Zheng, Z. Wang, Z. Wang, J. Yang, M. Chen, M. Qi, S. Ur Rehman, P.P. Shum and L. Zhu, *Advanced Materials Interfaces*, 8 (2021) 2001978.

6. S. Jun, S. Mahesula, T.P. Mathews, M.S. Martin-Sandoval, Z. Zhao, E. Piskounova and M. Agathocleous, *Cell metabolism*, 33 (2021) 1777.
7. X. Hu, P. Zhang, D. Wang, J. Jiang, X. Chen, Y. Liu, Z. Zhang, B.Z. Tang and P. Li, *Biosensors and Bioelectronics*, 182 (2021) 113188.
8. S.M.M. Dezfouli and S. Khosravi, *Indian Journal of Forensic Medicine and Toxicology*, 15 (2021) 2674.
9. D. Roosterman and G.S. Cottrell, *International Journal of Molecular Sciences*, 22 (2021) 604.
10. L. Liu, X. Zhang, Q. Zhu, K. Li, Y. Lu, X. Zhou and T. Guo, *Light: Science & Applications*, 10 (2021) 1.
11. Y.-S. Li, Q.-J. Li, W. Yang and X.-F. Gao, *Journal of fluorescence*, 27 (2017) 883.
12. R.F. Grace, P. Bianchi, E.J. van Beers, S.W. Eber, B. Glader, H.M. Yaish, J.M. Despotovic, J.A. Rothman, M. Sharma and M.M. McNaull, *Blood, The Journal of the American Society of Hematology*, 131 (2018) 2183.
13. C.S. Pundir, M. Malik and R. Chaudhary, *Microchemical Journal*, 146 (2019) 1102.
14. S. Khosravi and S.M.M. Dezfouli, *Journal of Critical Reviews*, 7 (2020) 275.
15. Y. Xie, X. Meng, Y. Chang, D. Mao, Y. Yang, Y. Xu, L. Wan and Y. Huang, *Composites Science and Technology*, 219 (2021) 109225.
16. H. Karimi-Maleh, Y. Orooji, F. Karimi, M. Alizadeh, M. Baghayeri, J. Rouhi, S. Tajik, H. Beitollahi, S. Agarwal and V.K. Gupta, *Biosensors and Bioelectronics*, 184 (2021) 113252.
17. X. Du, W. Tian, J. Pan, B. Hui, J. Sun, K. Zhang and Y. Xia, *Nano Energy*, 92 (2022) 106694.
18. V.H. Beretta, F. Bannoud, M. Insani, C.R. Galmarini and P.F. Cavagnaro, *Food chemistry*, 224 (2017) 201.
19. B. Cetin, G. Ucak Ozkaya, H. Uran and M.Z. Durak, *Journal of Food Safety*, 39 (2019) e12689.
20. T. Nimmanwudipong, N. Zhang, A. Gilbert, K. Yamada and N. Yoshida, *Journal of Analytical & Bioanalytical Techniques*, 7 (2015) 1000293.
21. S. Biagi, S. Ghimenti, M. Onor and E. Bramanti, *Biomedical Chromatography*, 26 (2012) 1408.
22. A. Zhu, R. Romero and H.R. Petty, *Analytical biochemistry*, 396 (2010) 146.
23. Q. Xue and E.S. Yeung, *Journal of Chromatography A*, 661 (1994) 287.
24. I. Kucherenko, Y.V. Topolnikova and O. Soldatkin, *TrAC Trends in Analytical Chemistry*, 110 (2019) 160.
25. S. Salehi, M. Kamali and M. Radgoodarzi, *Progress in Pediatric Cardiology*, 62 (2021) 101378.
26. M. Situmorang, J.J. Gooding, D.B. Hibbert and D. Barnett, *Electroanalysis: An International Journal Devoted to Fundamental and Practical Aspects of Electroanalysis*, 14 (2002)
27. F. Mirzaei, M. Mirzaei and M. Torkzadeh-Mahani, *Bioelectrochemistry*, 130 (2019) 107323.
28. M.A. Delavar and P. Karimian, *Pakistan Journal of Medical & Health Sciences*, 14 (2020) 1686.
29. H. Qi, Z. Hu, Z. Yang, J. Zhang, J.J. Wu, C. Cheng, C. Wang and L. Zheng, *Analytical chemistry*, (2022)
30. N. Gajovic, K. Habermüller, A. Warsinke, W. Schuhmann and F.W. Scheller, *Electroanalysis: An International Journal Devoted to Fundamental and Practical Aspects of Electroanalysis*, 11 (1999) 1377.
31. M.E. Ghica and C.M. Brett, *Electroanalysis: An International Journal Devoted to Fundamental and Practical Aspects of Electroanalysis*, 18 (2006) 748.
32. P.K. Brahman, N. Pandey, S.N. Topkaya and R. Singhai, *Talanta*, 134 (2015) 554.
33. M. Jin, Q. Dong, R. Dong and W. Jin, *Electrophoresis*, 22 (2001) 2793.
34. Y. Orooji, B. Tanhaei, A. Ayati, S.H. Tabrizi, M. Alizadeh, F.F. Bamoharram, F. Karimi, S. Salmanpour, J. Rouhi and S. Afshar, *Chemosphere*, 281 (2021) 130795.

35. G. Zhao and G. Liu, *Nanomaterials*, 9 (2019) 41.
36. B. He and H. Liu, *Sensors and Actuators B: Chemical*, 304 (2020) 127303.
37. T. Mushiana, N. Mabuba, A.O. Idris, G.M. Peleyeju, B.O. Orimolade, D. Nkosi, R.F. Ajayi and O.A. Arotiba, *Sensing and Bio-Sensing Research*, 24 (2019) 100280.
38. L.A. Goulart and L.H. Mascaro, *Electrochimica Acta*, 196 (2016) 48.
39. Y. Hao, F. Xiao, C. Xiao-Xia, Q. Jin-Li, G. Xiao-Ling, X. Na and G. Lou-Jun, *Chinese Journal of Analytical Chemistry*, 45 (2017) 713.
40. X. Jiang, W. Ding, Z. Lv and C. Rao, *Analytical Sciences*, (2021) 21P113.
41. M. Khosravi, *Open Access Macedonian Journal of Medical Sciences*, 8 (2020) 553.
42. S. Mehmood, R. Ciancio, E. Carlino and A.S. Bhatti, *International journal of nanomedicine*, 13 (2018) 2093.
43. J.-M. Yeh, K.-Y. Huang, S.-Y. Lin, Y.-Y. Wu, C.-C. Huang and S.-J. Liou, *Journal of Nanotechnology*, 2009 (2009) 1.
44. F. Wang, X. Liu and I. Willner, *Advanced Materials*, 25 (2013) 349.
45. K. Uematsu, M. Yamasaki, T. Hibi and H. Katano, *Analytical Sciences*, 28 (2012) 657.
46. L. Zhou, *International Journal of Electrochemical Science*, 16 (2021) 211043.
47. J. Wang, C. Liu and J. Hua, *International Journal of Electrochemical Science*, 16 (2021) 211016.
48. Y. Yang, N. Ma and Z. Bian, *International Journal of Electrochemical Science*, 14 (2019) 4095.
49. B. Risse, G. Stempfer, R. Rudolph, H. Möllering and R. Jaenicke, *Protein Science*, 1 (1992) 1699.
50. C.-J. Hsueh, J.H. Wang, L. Dai and C.-C. Liu, *Biosensors*, 1 (2011) 107.
51. S. Korkut, S. Göl and M.S. Kilic, *Electroanalysis*, 32 (2020) 271.
52. S. Tuncagil, C. Ozdemir, D.O. Demirkol, S. Timur and L. Toppare, *Food chemistry*, 127 (2011) 1317.
53. M. Malik, R. Chaudhary and C. Pundir, *International Journal of Applied Sciences and Biotechnology*, 7 (2019) 195.
54. L. Gilbert, S. Browning, A.T. Jenkins and J.P. Hart, *Microchimica Acta*, 170 (2010) 331.
55. N. Saifuddin, A. Raziah and A. Junizah, *Journal of Chemistry*, 2013 (2013) 1.
56. H. Malekzad, P.S. Zangabad, H. Mirshekari, M. Karimi and M.R. Hamblin, *Nanotechnology reviews*, 6 (2017) 301.
57. M. Khosravi, *Current Psychology*, 40 (2021) 5735.
58. P. Dsouza Priya Swetha and K. Sudhakara Prasad, *Electroanalysis*, 32 (2020) 2237.
59. J. Wang and P. Diao, *Electrochimica Acta*, 56 (2011) 10159.
60. P.K. Brahman, N. Pandey, J.V.S. Kumar, P. Somarouthu, S. Tiwari and K.S. Pitre, *Arabian Journal of Chemistry*, 9 (2016) S1897.
61. T. Pérez-Ruiz, C. Martínez-Lozano, V. Tomás and J. Fenoll, *Analytica chimica acta*, 485 (2003) 63.
62. T.-F. Zhang and L.P. Hager, *Archives of Biochemistry and Biophysics*, 257 (1987) 485.